

Effect of rare earth ion substitution on the magnetic and transport properties of $\text{Pr}_{0.7}\text{RE}_{0.04}\text{Sr}_{0.26}\text{MnO}_3$ (RE = Er^{3+} , Tb^{3+} and Ho^{3+})

N. Rama^{1,2,a}, J.B. Philipp³, M. Opel³, A. Erb³, V. Sankaranarayanan², R. Gross³, and M.S. Ramachandra Rao^{1,2,b}

¹ Materials Science Research Centre, Indian Institute of Technology Madras, Chennai – 600 036, India

² Department of Physics, Indian Institute of Technology Madras, Chennai – 600 036, India

³ Walther-Meissner-Institute, Bavarian Academy of Sciences, Walther-Meissner Str. 8, 85748, Garching, Germany

Received 7 March 2003 / Received in final form 4 February 2004

Published online 8 June 2004 – © EDP Sciences, Società Italiana di Fisica, Springer-Verlag 2004

Abstract. The effect of rare earth ion (RE = Er^{3+} , Tb^{3+} , Ho^{3+}) substitution in $\text{Pr}_{0.74}\text{Sr}_{0.26}\text{MnO}_3$ (PSMO(0.26)) on the magnetic and transport properties is reported. It is found that even for a small concentration of substitution of Pr^{3+} ions by Er^{3+} , Tb^{3+} , or Ho^{3+} ions there is a significant change in the transport and magnetic properties compared to the parent compound $\text{Pr}_{0.74}\text{Sr}_{0.26}\text{MnO}_3$. The observed changes are attributed to the increase in the average A-site disorder upon substituting smaller ions (ionic radius of $\text{Er}^{3+} = 1.062 \text{ \AA}$, $\text{Ho}^{3+} = 1.072 \text{ \AA}$, $\text{Tb}^{3+} = 1.095 \text{ \AA}$) in place of bigger Pr^{3+} ion (ionic radius = 1.179 \AA). The Ho^{3+} substituted sample was found to behave anomalously when compared to the other two rare earth ion-substituted (Tb^{3+} and Er^{3+}) samples. Such anomalous behaviour could most likely be caused by the magnetic coupling of the Ho and Mn ions.

PACS. 75.47.Lx Manganites

1 Introduction

The perovskite type Colossal Magnetoresistive (CMR) manganites of general composition $\text{R}_{1-x}\text{A}_x\text{MnO}_3$, where R is a rare earth ion and A is a divalent alkaline earth ion, exhibit an unusually strong interplay between orbital, lattice and spin degrees of freedom. At temperatures below their Curie temperature (T_C), optimally substituted ($x \sim 0.3\text{--}0.4$) manganites are ferromagnetic metals, while at higher temperatures, i.e. above T_C , they exhibit a paramagnetic insulating behaviour [1]. This generic behaviour, as well as the magnetoresistive effect which occurs near the metal-insulator transition (MIT), has been understood within the framework of the Zener double exchange (ZDE) model [2,3]. In this model, the creation of mixed valency of Mn ($\text{Mn}^{3+}/\text{Mn}^{4+}$) by hole doping at the rare-earth (RE) site plays an important role. The transfer (hopping) of an e_g electron between the neighbouring Mn^{3+} and Mn^{4+} ions through the Mn-O-Mn path, results in an effective ferromagnetic interaction due to strong on-site Hund's coupling.

When manganites are doped with aliovalent alkaline earth ions (valency 2+) like Ca^{2+} , Sr^{2+} etc. in the A-site, the carrier concentration as well as the average A-site ionic

radius changes. On the other hand when isovalent rare earth ions (valency 3+) like Er^{3+} , Tb^{3+} or Y^{3+} are substituted in the A-site, only the average A-site ionic radius changes.

The change in the A-site ionic radii affects the ferromagnetic exchange which causes a change in the ferromagnetic transition temperature as well as the resistivity and magnetoresistance [4,5]. The above scenario is related to the change of the tolerance factor (t) and the increase in A-site disorder causing a tilt and/or rotation of the oxygen octahedra around the Mn ions. This in turn results in a change of the Mn-O-Mn bond angles away from 180° and hence a reduction of the hopping matrix element of the e_g electrons and narrowing of the effective electronic bandwidth [6–9]. The average A-site disorder is characterized by a parameter $\langle\sigma^2\rangle$ given by [10]

$$\langle\sigma^2\rangle = \sum_i y_i r_i^2 - \left(\sum_i y_i r_i \right)^2 \quad (1)$$

where r_i is the ionic radii of the A site ion of concentration y_i .

In a recent work [11], it has been shown that the substitution of La^{3+} by Ho^{3+} and Y^{3+} ions in $\text{La}_{0.7}\text{Ca}_{0.3}\text{MnO}_3$ (LCMO) yields interesting results. Upon substitution of Ho^{3+} ions at the La-site in LCMO, the resistivity decreases dramatically compared to that of Y^{3+} substituted

^a e-mail: rama@physics.iitm.ac.in

^b e-mail: msrrao@iitm.ac.in

LCMO for similar concentration levels. Ho^{3+} and Y^{3+} ions have the same ionic radii and hence, the observed change in resistivity for the same concentration of the dopant was attributed to the magnetic nature of the Ho^{3+} ion. Magnetization studies unequivocally proved an increase in magnetic moment per formula unit in the Ho^{3+} substituted compounds indicating a coupling between the Ho^{3+} and $\text{Mn}^{3+/4+}$ moments. This work has prompted us to study the effect of the substitution of magnetic rare-earth ions in a manganite such as $\text{Pr}_{0.74}\text{Sr}_{0.26}\text{MnO}_3$ (PSMO (0.26)), which already has a magnetic ion (Pr^{3+}) in its lattice. Such a study — rare earth substitution at the Pr site in PSMO system — has not been attempted in the manganites to the best of our knowledge.

In this paper, we present the effect of the substitution of Er^{3+} , Ho^{3+} and Tb^{3+} ions on the transport and magnetic properties of $\text{Pr}_{0.74}\text{Sr}_{0.26}\text{MnO}_3$ (PSMO (0.26)). Since within the framework of the ZDE model the Mn^{4+} concentration is one of the factors that determines T_C , we have substituted the PSMO(0.26) system such that the resulting compounds have the same Mn^{4+} concentration with different $\langle\sigma^2\rangle$ values (Tab. 1).

2 Experimental techniques

In order to exclusively study the effect of A-site disorder on magnetic and electrical transport properties, it is desirable that the tolerance factor of the RE-substituted PSMO(0.26) compositions has to be kept constant. This was achieved in the following way. The tolerance factor of $\text{Pr}_{0.7}\text{Er}_{0.04}\text{Sr}_{0.26}\text{MnO}_3$ was calculated (0.917) and the concentrations of the other two substituents (Ho^{3+} and Tb^{3+}) were adjusted such that all three RE-substituted PSMO compositions had the same tolerance factor equal to 0.917. Thus the nominal compositions of the (Ho^{3+} and Tb^{3+}) are $\text{Pr}_{0.699}\text{Ho}_{0.041}\text{Sr}_{0.26}\text{MnO}_3$ and $\text{Pr}_{0.697}\text{Tb}_{0.043}\text{Sr}_{0.26}\text{MnO}_3$ respectively. These compounds were prepared along with the unsubstituted PSMO (0.26) ($t = 0.919$) composition for comparison.

Polycrystalline samples of the composition $\text{Pr}_{0.7}\text{RE}_{0.04}\text{Sr}_{0.26}\text{MnO}_3$ (RE = Er^{3+} , Ho^{3+} , Tb^{3+}) were prepared by the conventional solid-state method.

Stoichiometric amounts of preheated Pr_6O_{11} , Er_2O_3 , Ho_2O_3 , Tb_4O_7 , SrCO_3 and MnO_2 were weighed and mixed thoroughly in an agate mortar and calcined in an alumina crucible at 950°C for 24 h. The calcined powders were reground and heated again at 1250°C for another 24 h. The resultant powder was then pressed into pellets of 10 mm diameter and sintered in air at 1350°C for 24 h.

X-ray diffraction (XRD) of the samples was performed using Cu-K_α radiation using a two-circle diffractometer (Rich-Seifert, Germany). The electrical resistivity of the samples was measured using the standard linear four-probe technique in the temperature range of 2 K to 400 K using an Oxford continuous flow cryostat. Magnetization measurements were carried out using a SQUID magnetometer (Quantum design MPMS XL) in the same temperature range in a field cooled mode of 1000 Oe on powdered samples.

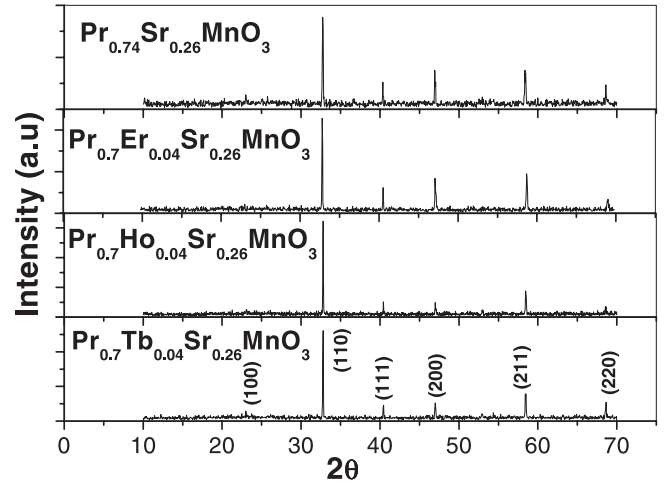


Fig. 1. X-Ray diffraction pattern for $\text{Pr}_{0.74}\text{Sr}_{0.26}\text{MnO}_3$ and the rare earth substituted samples $\text{Pr}_{0.7}\text{RE}_{0.04}\text{Sr}_{0.26}\text{MnO}_3$ (RE = Er, Ho and Tb). All the samples could be indexed to a pseudo-cubic structure.

Table 1. Lattice parameter, average A site disorder, maximum resistivity value, activation energy (from high temperature fits) and the low temperature fit parameters; unsub: unsubstituted; Tb^{3+} sub: Tb^{3+} substituted sample; Ho^{3+} sub: Ho^{3+} substituted sample and Er^{3+} sub: Er^{3+} substituted sample.

| Compound | a (Å) | $\langle\sigma^2\rangle$ (Å ²) $\times 10^{-3}$ | ρ_{max} (Ωcm) | E_A (eV) | p | ρ_{LT} (Ωcm) |
|----------------------|------------|---|-----------------------|---------------|------|----------------------|
| unsub PSMO(0.26) | 3.87 | 3.66 | 1.00 | 0.14 | 2.56 | 0.02 |
| Tb^{3+} sub | 3.86 | 4.06 | 15.14 | 0.15 | 3.58 | 0.47 |
| Ho^{3+} sub | 3.86 | 4.34 | 18.74 | 0.19 | 3.24 | 0.75 |
| Er^{3+} sub | 3.86 | 4.44 | 312.76 | 0.21 | 3.40 | 9.87 |

3 Results and discussion

X-ray diffraction pattern of the samples are shown in Figure 1. All the samples could be indexed to a pseudo-cubic structure. The corresponding lattice constants are listed in Table 1.

3.1 Resistivity measurements

The temperature dependence of electrical resistivity of the four samples is shown in Figure 2. The metal-insulator (MI) transition, a characteristic feature of the substituted manganites, is clearly seen for all samples.

Furthermore, it is evident that all RE substituted samples show much higher resistivity over the entire temperature range compared to unsubstituted PSMO (0.26). We find that the resistivity value at the maximum (corresponding to a temperature referred to as T_P) in the resistivity versus temperature curve of the substituted samples is largest for the Er^{3+} substituted PSMO (0.26) (maximum $\langle\sigma^2\rangle$), and lowest for the Tb^{3+} substituted

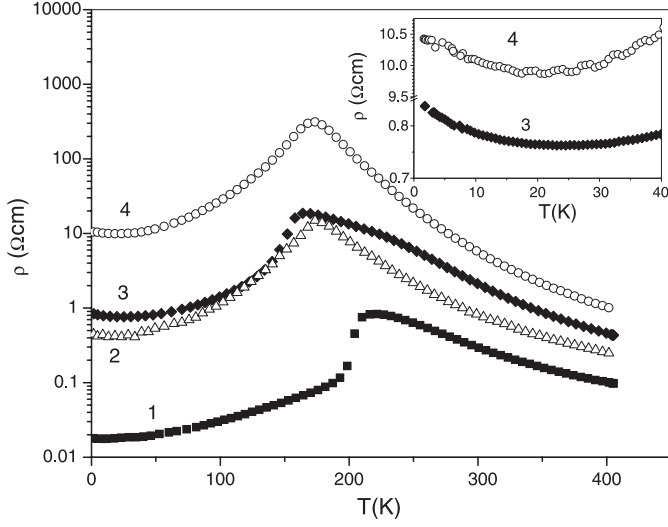


Fig. 2. Resistivity versus temperature curves for $\text{Pr}_{0.74}\text{Sr}_{0.26}\text{MnO}_3$ (1) and $\text{Pr}_{0.7}\text{RE}_{0.04}\text{Sr}_{0.26}\text{MnO}_3$ (RE = Tb(2), Ho(3) and Er(4)). The inset shows the low temperature resistivity upturn in Ho^{3+} and Er^{3+} substituted samples.

PSMO (0.26) sample (minimum $\langle\sigma^2\rangle$) thus scaling with A-site disorder as calculated using equation (1) (see Tab. 1). The sharp drop in the resistivity with temperature that is observed for the pure PSMO (0.26) just below the MI transition is absent in the substituted samples. This suggests that the MI transition in the substituted samples is much more gradual than in the pure sample. This gradual transition may occur due to the onset of percolative transport behaviour [12]. At temperatures above T_P , the temperature dependence of resistivity can be described within the adiabatic polaron hopping model [13]

$$\rho(T) = \rho_0 T \exp\left(\frac{E_A}{k_B T}\right). \quad (2)$$

The values of activation energy (E_A) obtained for various substituted compounds by fitting the experimental data with equation (2) (see Tab. 1 and Fig. 3) is found to increase with increase in A-site disorder.

It is interesting to note that among the rare earth substituted compounds, the fitting range (274 K to 400 K) is lower for $\text{Pr}_{0.7}\text{Ho}_{0.04}\text{Sr}_{0.26}\text{MnO}_3$ substituted sample than that (248 K to 400 K) for the $\text{Pr}_{0.7}\text{Tb}_{0.04}\text{Sr}_{0.26}\text{MnO}_3$ substituted sample due to the presence of a kink in the high temperature resistivity (marked by a vertical arrow in Figure 3 in the plot corresponding to the $\text{Pr}_{0.7}\text{Ho}_{0.04}\text{Sr}_{0.26}\text{MnO}_3$ data). It is observed that this kink is suppressed upon application of a magnetic field (Fig. 4) pointing to the presence of magnetic correlations even above T_C for the Ho^{3+} sample.

All the samples exhibit a minimum in low temperature resistivity around 30 K. The upturn below 30 K was found to be insensitive to the substitutions at the rare earth ion site and occurs more or less at the same temperature in all the samples including the unsubstituted compound. This behaviour could be due to intergranular tunneling between grains [14,15]. The low temperature dependence

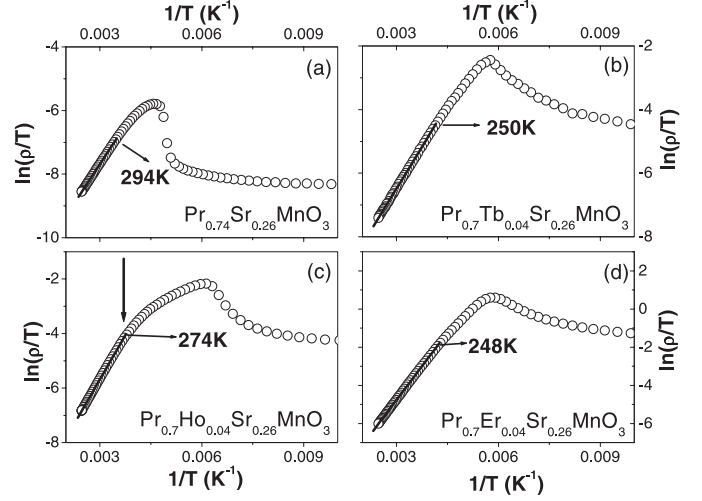


Fig. 3. Fit (solid lines) to the adiabatic polaron hopping model for $\text{Pr}_{0.74}\text{Sr}_{0.26}\text{MnO}_3$ (a) and $\text{Pr}_{0.7}\text{RE}_{0.04}\text{Sr}_{0.26}\text{MnO}_3$ (RE = Tb^{3+} , Ho^{3+} and Er^{3+}) compounds (b,c and d respectively). For the fits, a temperature interval extending from 294 K, 250 K, 274 K, 248 K to 400 K, respectively, was used. The vertical arrow in (c) indicates the deviation from the linear behaviour which can be due to the persistence of magnetic correlations above T_C in the Ho^{3+} -substituted compound.

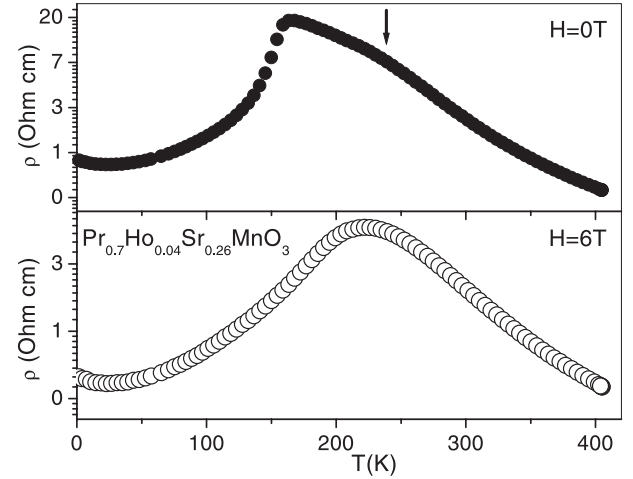


Fig. 4. Resistivity at 0 T (upper panel) and at 6 T (lower panel) for $\text{Pr}_{0.7}\text{Ho}_{0.04}\text{Sr}_{0.26}\text{MnO}_3$ sample. The kink in the resistivity is indicated by the arrow. It is seen that, the kink is suppressed on application of a magnetic field possibly showing its magnetic origin.

of the resistivity could be fitted to an expression of the form

$$\rho(T) = \rho_{LT} + \rho_1 T^p \quad (3)$$

from 40 K to 100 K (Fig. 5). It is seen that the exponent p is higher for the substituted samples as compared to the unsubstituted samples. For the unsubstituted sample p is found to be 2.5, which is usually observed for conventional manganites and is attributed to half metallic behaviour [16,17]. However, for the substituted samples we obtain an exponent ranging between 3 and 4. This suggests a more complex nature of the electrical transport in

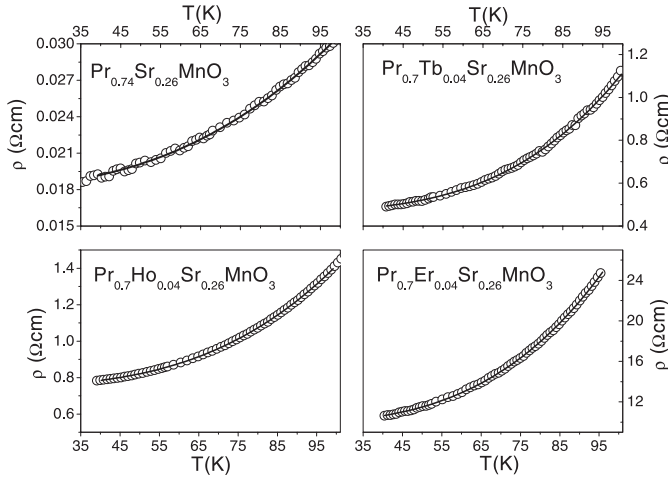


Fig. 5. Resistivity versus temperature curves in the low temperature regime. Also shown are the fits to the expression $\rho(T) = \rho_{LT} + \rho_1 T^p$. The open symbols and the solid line represent data points and the fitting curve, respectively.

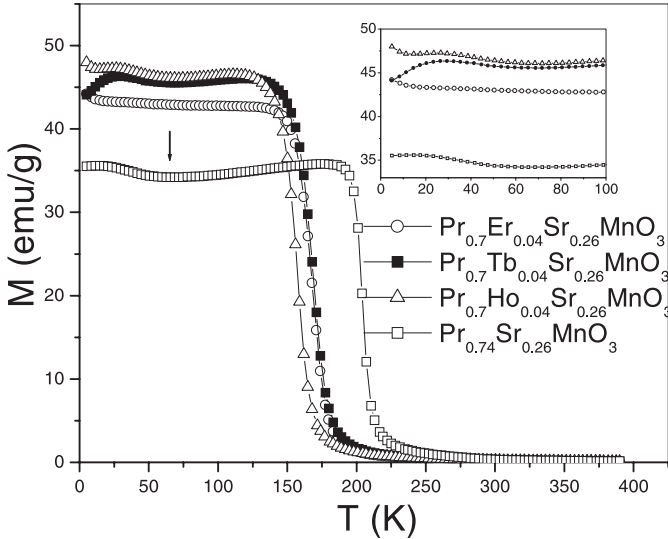


Fig. 6. Temperature dependence of magnetization in a field of 1000 Oe. The arrow indicates the onset of Pr sublattice ordering induced by the molecular field of Mn. Inset shows the low temperature magnetic behaviour.

the RE substituted samples. It is also seen that the fitting parameter, ρ_{LT} also increases with increase in A-site disorder.

3.2 Magnetization measurements

Figure 6 shows the magnetization versus temperature plots for all the four samples. It is seen that the magnetization curves show a minimum around 60 K, which is attributed to the Pr^{3+} sublattice ordering induced by the molecular field of Mn ions [18] as seen from neutron diffraction [19]. However, in the Er^{3+} substituted PSMO (0.26) sample the magnetization minimum is not seen even though it is clearly seen in the Ho^{3+} substituted

sample although they have comparable $\langle \sigma^2 \rangle$ values. Below 25 K, it is seen that the magnetization of the Ho^{3+} substituted sample and the Er^{3+} substituted sample increases while that of the Tb^{3+} substituted sample decreases (Inset in Fig. 6). A similar behaviour is also seen in $\text{La}_{0.625}\text{Ho}_{0.075}\text{Ca}_{0.3}\text{MnO}_3$ [11] and Tb^{3+} and Ho^{3+} doped $\text{Pr}_{0.7}\text{Sr}_{0.3}\text{MnO}_3$. Hence this behaviour may be attributed to the polarization of the magnetic rare earth sublattice induced by the molecular field of Mn ions. The decrease in magnetization observed in the Tb^{3+} substituted compound may also be due to the magnetic anisotropy of Tb usually observed at low temperatures [20] or due to a canting of Mn spins as observed in $\text{Nd}_{0.7}\text{Sr}_{0.3}\text{MnO}_3$ [21]. Neutron diffraction measurements have been planned to address these issues.

3.3 Anomalous behaviour of Ho^{3+} substituted PSMO (0.26)

From the discussion above it is seen that though the peak resistivity values of all the samples scale with $\langle \sigma^2 \rangle$, resistivity of the Ho^{3+} substituted sample is nearly the same as that of the Tb^{3+} substituted sample even though it has higher A-site disorder. This observation coupled with the presence of the kink in the high temperature resistivity for the Ho^{3+} substituted sample alone, possibly due to the existence of magnetic clusters above T_C suggests an anomalous behaviour of the Ho^{3+} substituted sample. The anomalous behaviour of Ho^{3+} substituted sample may be due to the following reason. Recent high field magnetization measurements have revealed a coupling between the moments of the Ho and Mn ions [11] in $\text{La}_{0.7}\text{Ca}_{0.3}\text{MnO}_3$. Moreover, neutron diffraction measurements show that Pr moments order ferromagnetically, possibly due to a coupling between Pr and Mn moments [19,21]. This coupling may be weakened by the increase in A-site disorder (higher $\langle \sigma^2 \rangle$) as evidenced by the absence of the magnetization minimum around 60 K for the Er^{3+} substituted sample. The magnetization minimum however, is observed in the Ho^{3+} substituted sample though it has a $\langle \sigma^2 \rangle$ comparable to that of the Er^{3+} substituted sample. In this case the effect of A-site disorder may be offset by the tendency of Ho moments to couple with those of Mn. Further measurements are however needed to understand these effects better.

4 Conclusions

We have measured the electrical transport and magnetic properties of RE substituted $\text{Pr}_{0.7}\text{RE}_{0.04}\text{Sr}_{0.26}\text{MnO}_3$ (RE = Tb^{3+} , Ho^{3+} and Er^{3+}). Our study shows that even for small substitution concentrations such as 0.04 there is a change in the transport and magnetic properties of the PSMO (0.26) manganite system. It is interesting to observe that the Ho^{3+} substituted sample behaves anomalously compared to the Er^{3+} and Tb^{3+} substituted samples both in terms of magnetism and transport. This anomalous behaviour of the Ho^{3+} substituted

in $\text{Pr}_{0.7}\text{RE}_{0.04}\text{Sr}_{0.26}\text{MnO}_3$ most likely arises from a coupling between the magnetic moments of the Ho^{3+} and $\text{Mn}^{3+/4+}$ ions. The reason as to why Ho^{3+} alone should couple and not Er^{3+} and Tb^{3+} is at present not clear and microscopic measurements are needed to understand these better and are being carried out.

MSR would like to thank BMBF (Bundesministerium für Bildung und Forschung), Germany for the award of a joint collaborative Indo-German project.

References

1. R. von Helmolt, J. Wecher, B. Holzapfel, L. Schultz, K. Samwer, Phys. Rev. Lett. **71**, 2331 (1993)
2. C. Zener, Phys. Rev. B **82**, 403 (1951); P.-G. de Gennes, Phys. Rev. **118**, 141 (1960)
3. P.W. Anderson, H. Hasegawa, Phys. Rev. **100**, 675 (1955)
4. C.N.R. Rao, A.K. Cheetham, R. Mahesh, Chem. Mater. **8**, 2421 (1996)
5. A.P. Ramirez, J. Phys: Condens. Matter **9**, 8171 (1997)
6. H.Y. Hwang, S.-W. Cheong, P.G. Radaelli, M. Marezio, B. Batlogg, Phys. Rev. Lett. **75**, 914 (1995)
7. J.R. Sun, G.H. Rao, J.K. Liang, Appl. Phys. Lett. **70**, 1900 (1997)
8. J. Fontcuberta, B. Martinez, A. Seffar, S. Pinol, J.L. Garcia-Munoz, X. Obradors, Phys. Rev. Lett. **76**, 1122 (1996)
9. Z.B. Guo, N. Zhang, W.P. Ding, W. Yang, J.R. Zhang, Y.W. Du, Solid State Commun. **100**, 769 (1996)
10. L.M. Rodriguez-Martinez, P. Attfield, Phys. Rev. B **54**, R15622 (1996)
11. V. Ravindranath, M.S. Ramachandra Rao, G. Rangarajan, Yafeng Lu, J. Klein, R. Klingeler, S. Uhlenbruck, B. Büchner, R. Gross, Phys. Rev. B **63**, 184434 (2001)
12. E. Dagotto, H. Takashi, A. Moreo, Phys. Rep. **344**, 1 (2001)
13. T. Holstein, Ann. Phys. **8**, 343 (1959)
14. E. Rozenberg, M. Auslender, I. Felner, G. Gorodetsky, J. Appl. Phys. **88**, 2578 (2000)
15. M.I. Auslender, E. Rozenberg, A.E. Kar'kin, B.K. Chaudhuri, G. Gorodetsky, J. Alloys Compounds **326**, 81 (2001)
16. X. Wang, X.G. Zhang, Phys. Rev. Lett. **82**, 4276 (1999)
17. P. Schiffer, A.P. Ramirez, W. Bao, S.-W. Cheong, Phys. Rev. Lett. **75**, 3336 (1995)
18. J.G. Park, M.S. Kim, H.-C. Ri, K.H. Kim, T.W. Noh, S.-W. Cheong, Phys. Rev. B **60**, 14804 (1999)
19. Z. Jirak, S. Vratislav, J. Zajicek, Phys. Status Solidi (a) **52**, K39 (1979)
20. *Ferromagnetic Materials*, edited by E.P. Wohlfarth, Vol. 1 (North-Holland, 1980)
21. Junghwan Park, M.S. Kim, J.-G. Park, I.P. Swainson, H.-C. Ri, H.J. Lee, K.H. Lee, K.H. Kim, T.W. Noh, S.W. Cheong, Changhe Lee, J. Korean Phys. Soc. **36**, 412 (2000)